

Radiation damage and trapping of helium in HOPG-graphite

G. Ramos *, B.M.U. Scherzer

Max-Planck Institut für Plasmaphysik, EURATOM Association, Boltzmannstrasse 2, 85748 Garching bei München, Germany

Rutherford backscattering analysis in channeling geometry has been used to measure the formation and annealing of radiation damage in highly oriented pyrolytic graphite (HOPG) implanted with 20 keV helium ions. The number of displaced atoms per incoming ion at room temperature was found to be more than four times greater for helium ions than for deuterium of equal damage profile and much greater than model calculations. On the annealing of HOPG implanted with a low fluence of helium up to 800 K an increase of the disorder in the implanted region is observed which is attributed to the formation of blisters at the surface. The desorption of helium implanted at 300 K was investigated by ion beam analysis using the nuclear reaction $^3\text{He}(\text{D}, \text{p})\alpha$. Low fluence implanted helium ($2 \times 10^{15} \text{ He/cm}^2$) did not desorb below 950 K.

1. Introduction

Graphite and carbon-based materials are favorite candidate first wall materials for plasma fusion devices. Extensive studies of the implantation of energetic plasma components in graphite have been made in the past [1,2]. Nevertheless some phenomena are still not fully understood, e.g. the trapping and desorption of light ions in graphite and its connection with radiation damage.

In recent years structural changes and defect structures due to the implantation of intermediate energy (25 keV) helium and deuterium ions in HOPG have been extensively studied using transmission electron microscopy (TEM) [3,4]. In these studies the critical fluences for the crystalline to amorphous transition of HOPG bombarded at different temperatures as well as conditions for the occurrence of the observed defects (i.e. lenticular openings, twins and spherical bubbles) were determined.

Rutherford backscattering spectroscopy in channeling geometry (RBS-C) has been applied to pseudocrystalline materials such as highly oriented pyrolytic graphite (HOPG) [5]. Recently RBS-C has been applied to study the relation between radiation damage and trapping of deuterium in HOPG – graphite [6]. It was found that deuterium damage in HOPG observed with RBS-C saturates at fluences far below those at which amorphisation is observed in TEM. Further, deuterium damage was found to be ten times higher than predicted by TRIM.SP [7] calculations. Since hy-

drogen interacts chemically with carbon, the C–H bonds may be important for the production and stabilisation of damage. The mechanism of this interaction, however, is not clear.

Therefore, our aim was to study the production of damage due to the implantation of a chemically inert ion (helium) in HOPG and its influence on the annealing processes in comparison with the behavior of deuterium.

2. Experimental details

In the present work HOPG samples (ZYA-grade from Union Carbide (USA) and pseudo single crystals from Le Carbone-Lorraine (France)) with the *c*-axis normal to the surface were used. The samples were prepared by repeated stripping with adhesive tape.

The experimental setup is described elsewhere [6,8]. The channeling analysis as well as the implantations were made parallel to the *c*-axis. For high temperature implantations as well as for thermal annealing and release experiments the sample could be heated ohmically up to 1000 K. The temperature was controlled by a thermocouple attached to the front surface of the sample. The implantations were done at 300, 573 and 720 K with 20 keV helium ions with fluences ranging from 10^{14} to 10^{17} ions/ cm^2 . During implantation the beam was swept vertically over the beam spot to assure uniform implantation.

For samples implanted at 300 K the analysis was carried out mainly with $^4\text{He}^+$ with energies between 1 and 2 MeV. For samples implanted at higher temperatures only hydrogen beams with energies between 400

* Corresponding author, phone +49 89 3299 1266, fax +49 89 3299 2591.

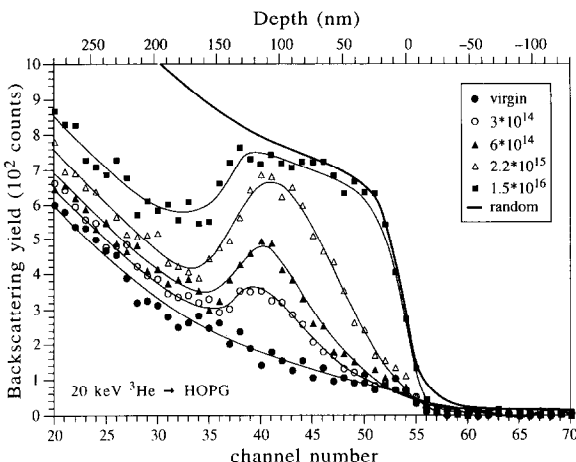


Fig. 1. Rutherford backscattering spectra for the implantation of 20 keV ^3He ions at 300 K parallel to the c -axis. The spectra were obtained with 1 MeV ^3He ions.

and 600 keV were used, because excessive damage was produced by the analysing ^4He beam. The trapping and release of ^3He ions in HOPG was monitored by means of the nuclear reaction $^3\text{He}(\text{D}, \text{p})\alpha$. Additionally selected samples were analysed after implantation or annealing by scanning electron microscopy (SEM).

3. Results and discussion

3.1. Helium damage in HOPG

Fig. 1 shows a series of channeling spectra for the implantation of ^3He ions with 20 keV at 300 K. These spectra were obtained with 1 MeV ^3He ions. Even for the smallest fluence shown ($3 \times 10^{14} \text{ He/cm}^2$) a damage peak at a depth around 110 nm is observed. With increasing fluence the peak grows in height until its maximum reaches the random yield at $2.2 \times 10^{15} \text{ He/cm}^2$. This fluence will be referred to as "beginning of amorphisation". With increasing fluences the peak spreads preferentially to the surface, while the dechan-

neling yield (yield at depths $> 170 \text{ nm}$) saturates. At a fluence of $1.5 \times 10^{16} \text{ He/cm}^2$ the damage peak has extended to the surface. This fluence will be referred to as "completion of amorphisation". At even higher fluences the channeling does not change further, except in cases where new surface is exposed due to flaking.

At 570 K the damage production proceeds at a smaller rate but with similar characteristics as found at 300 K. This indicates partial annealing of damage during implantation.

At 720 K the damage production rate is again reduced compared to 570 K. The damage peak, however, extends from the surface up to a depth of 170 nm from the very beginning of implantation. Thus, at this temperature, no definite beginning of amorphisation, in the sense used at 300 K, can be defined. Further, due to the occurrence of flaking between 1 and $2 \times 10^{16} \text{ He/cm}^2$ no gradual transition towards completion of amorphisation could be observed. Data for beginning and completion of amorphisation are summarised in Table 1 together with fluences for crystalline to amorphous transition taken from reference [3]. Only values for ^4He ions can be compared. The TEM results for the crystalline to amorphous transition are higher than RBS-C values for completion of amorphisation. This discrepancy is more pronounced at 720 K.

Integral damage is obtained from the RBS-C spectra by integrating the yield of the damage peak after subtracting the dechanneled yield, as described in Ref. [8]. For these calculations the damage is assumed to consist of interstitial atoms.

Fig. 2 shows the computed integral damage for the implantation of the helium isotopes ^4He and ^3He at 300 K together with data for the implantation of 8 keV D^+ taken from reference [6]. The helium ion energy was selected so that the damage profile was almost equal to the damage profile due to the implantation of deuterium ions used in reference [6] (8 keV D^+). Damage due to the implantation of ^4He ions grows faster and saturates earlier than damage due to ^3He ions or damage due to deuterium ions.

Table 1

Fluences for beginning and completion of amorphisation for damage due to He ions implanted at different temperatures together with fluences for crystalline to amorphous transition taken from ref. [3]

Ion species	Temperature [K]	Amorphisation (RBS-C)		Crystalline to amorphous transition (TEM)
		Beginning	Completion	
20 keV $^4\text{He}^+$	300	10^{15}	$1-1.5 \times 10^{16}$	2×10^{16}
	720	not defined	$\sim 3 \times 10^{16}$	10^{18}
20 keV $^3\text{He}^+$	300	2.2×10^{15}	$1.5-2 \times 10^{16}$	
	573	$8-9 \times 10^{15}$	2.5×10^{16}	
	720	not defined	$\sim 4 \times 10^{16}$	

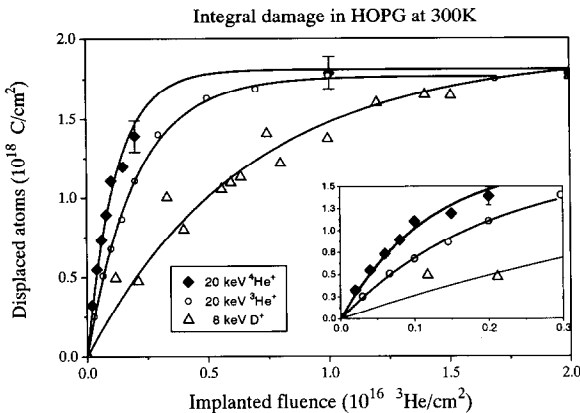


Fig. 2. Integral damage due to the implantation of ⁴He, ³He and D ions at 300 K in dependence of the implanted fluence. The insert is a blow-up of the low fluence part.

The amount of displaced atoms per incoming ion is computed from the initial slope of the integral damage curves. These values for both He isotopes together with data taken from reference [6], and calculations using TRIM.SP [7] are shown in Table 2. For the calculations a displacement energy of 25 eV [9] is assumed, the Kr-C potential was used as projectile-target interaction potential, and the energy loss was calculated using Lindhard/Scharff and Oen-Robinson stopping powers at equal parts. The results indicate that also in the absence of chemical projectile-target interaction the damage production is higher than expected from collision theory. Our RBS-C results are between 8 (for ³He ions) and 15 (for ⁴He ions) times greater than TRIM.SP results.

For the interpretation of the RBS-C spectra two aspects must be considered:

(1) Due to its polycrystalline character an increase of the mean tilt angle of individual crystallites around the *c*-axis (mosaic spread) results in an increase of the backscattering yield [5]. We found experimentally for 1 MeV He-ions that a tilt of the analysing beam for about 1° with respect to the *c*-axis is sufficient to obtain random yield. Due to the implantation of D in

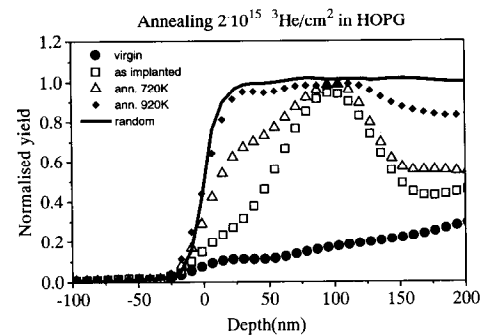


Fig. 3. RBS-C spectra for the annealing of damage due to the implantation of 2×10^{15} ³He/cm² at 300 K. The annealing time was 5 min at each temperature. The RBS-C spectra were obtained with 1 MeV ⁴He ions.

HOPG, Siegele et al. [6] found splitting of individual crystallites into smaller ones and a tilting of these subcrystallites for about 1 degree with respect to the bulk *c*-axis. In the case of helium implantation the reduction of the crystallite size was observed by laser Raman spectroscopy [10]. Although there is no TEM evidence in the latter case, crystal splitting can be assumed to play an important role in He implantation.

(2) Further, the presence of strain can induce an increased backscattering yield in crystalline materials [11] although the material is not yet amorphised. In HOPG the occurrence of strain due to the production of defects cannot be excluded. It has been suggested that strain may be the reason for flaking in helium implanted graphite [12]. Both aspects must be considered in the interpretation of our RBS-C results. At 300 K the splitting and tilting of crystallites can be assumed to play the major role.

3.2. Annealing of damage

The evolution of disorder in the implanted region for the thermal annealing at 720 and 920 K of a HOPG sample implanted with 2×10^{15} ³He/cm² at 300 K is shown in Fig. 3. This fluence was selected because at this fluence the beginning of amorphisation is not yet reached.

Up to 600 K no change of the damage profile was observed. At 720 K the disorder in the damaged region grows towards the surface together with an increase of the dechanneling level. This behavior is more pronounced after annealing at 920 K, where the disorder reaches the surface. The increase of disorder in the implanted region can be attributed to the formation of blisters at the surface, as evidenced by SEM.

In contrast, damage due to the implantation of deuterium at fluences where amorphisation (as observed by TEM) has not yet occurred, starts to anneal

Table 2

Comparison between the number of displaced atoms per incoming ion for the implantation of ⁴He, ³He and D at 300 K and TRIM.SP calculations. Data for deuterium taken from ref. [6]

Displaced atoms per incoming ion	Implanted ion		
	⁴ He+ (20 keV)	³ He+ (20 keV)	D+ (8 keV)
RBS-C	1160	490	256
TRIM.SP	77	59	20.5

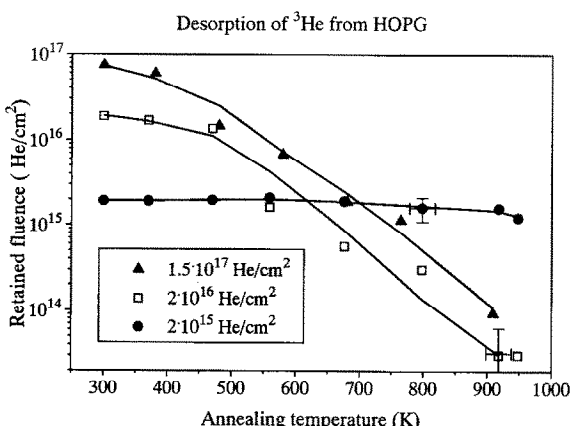


Fig. 4. Desorption of ${}^3\text{He}$ from HOPG for three fluences (2×10^{15} , 2×10^{16} and $1.5 \times 10^{17} \text{ He/cm}^2$) implanted at 300 K with 20 keV for isochronally annealing for 5 min at each temperature.

already at 500 K [13]. Evidence of annealing of deuterium damage is also observed by RBS-C [8]. Further, the reduction of He-damage due to thermal annealing has been observed by laser Raman spectroscopy [14]. The observed increase of disorder in RBS-C (and the formation of blisters during annealing) could be explained by the assumption of gas bubble coalescence in the implanted layer and a consequent expansion with increasing temperature, which produces strain and blisters. This assumption, however, is in contradiction with the desorption behavior of helium from various graphites [15–17]. According to these experiments helium desorbs between 500 and 700 K.

In order to verify if this desorption behavior also holds for HOPG, the thermal desorption at three selected fluences was investigated. The fluences were chosen according to three representative damage stages according to Fig. 1: $2 \times 10^{15} \text{ He/cm}^2$ (beginning of amorphisation), $2 \times 10^{16} \text{ He/cm}^2$ (completion of amorphisation) and $1.5 \times 10^{17} \text{ He/cm}^2$ (amorphous).

Fig. 4 shows the amount of retained helium (implanted at 300 K in HOPG after annealing at temperatures between 300 and 950 K for the three selected fluences (2×10^{15} and $1.5 \times 10^{17} \text{ He/cm}^2$) occurs between 500 and 700 K, and at 950 K almost all helium is desorbed. This behavior is in good agreement with earlier TDS experiments in graphite [15–17].

The desorption behavior at the smallest fluence ($2 \times 10^{15} \text{ He/cm}^2$) is quite unexpected: up to 950 K no significant desorption is observed. This suggests that the blisters found after our annealing experiments are gas-filled. The SEM pictures suggest the following desorption mechanism: at fluences of the order of beginning of amorphisation helium coalesces to bubbles due

to annealing. With increasing temperature bubbles develop to blisters, but the gas pressure is not sufficient to produce open blisters. At higher fluences (of the order of completion of amorphisation) with increasing temperature the gas pressure is sufficient to produce open blisters, and so the gas can escape. So, this suggests that there is a connection between the damage stage of the material and the desorption behaviour of helium.

4. Conclusions

The damage due to the implantation of 20 keV He ions in HOPG, as seen by RBS-C, is greater than found by TEM or predicted by collision theory. Splitting and tilting of crystallites with tilt angles greater than 1° and the production of strain are considered to be the principal reasons.

Damage due to the implantation of helium with a fluence below the beginning of amorphisation could not be annealed.

Helium implanted with fluences greater than those corresponding to completion of amorphisation desorbs between 500 K and 950 K, while helium implanted with fluences about the beginning of amorphisation does not desorb up to 950 K.

Acknowledgement

One of us (G. Ramos) wants to thank the Universidad Nacional Autonoma de Mexico for economical support with a scholarship during the realisation of this work.

References

- [1] W. Möller, J. Nucl. Mater. 162–164 (1989) 138.
- [2] W. Möller, J. Roth, NATO ASI Series B:Physics, vol. 131, eds. D.E. Post and R. Behrisch (Plenum Press, New York, 1986) 439.
- [3] K. Niwase, T. Tanabe, M. Sugimoto and F.E. Fujita, J. Nucl. Mater. 155–157 (1988) 303.
- [4] K. Niwase, T. Tanabe, M. Sugimoto and F.E. Fujita, J. Nucl. Mater. 162–164 (1989) 856.
- [5] B.S. Elman, G. Braunstein, M.S. Dresselhaus, G. Dresselhaus, T. Venkatesan and B. Wilkens, J. Appl. Phys. 56 (1984) 2114.
- [6] R. Siegele, J. Roth, B.M.U. Scherzer and S.J. Pennycook, J. Appl. Phys. 73 (1993) 2225.
- [7] W. Eckstein, Computer Simulation of Ion-solid Interactions, Springer Series in Mater. Sci., vol. 10 (Springer, 1991).
- [8] R. Siegele, PhD Thesis, Technische Universität München (1991) in German.

- [9] D.T. Eggen, report NAA-SR-69 (1950);
J.H.W. Simmons, *Irradiation Damage in Graphite* (Pergamon Press, New York, 1965).
- [10] K. Niwase and T. Tanabe, *J. Nucl. Mater.* 190 (1990) 106.
- [11] J.A. Edmond and R.F. Davis, S.P. Withrow and K.L. More, *J. Mater. Res.* 3 (1988) 321.
- [12] Y. Higashida and K. Kamada, *J. Nucl. Mater.* 73 (1978) 30.
- [13] K. Niwase, T. Tanabe, I. Tanaka, *J. Nucl. Mater.* 191–194 (1992) 335.
- [14] K. Niwase, private communication.
- [15] H. Atsumi, S. Yamanaka, P. Son and M. Miyake, *J. Nucl. Mater.* 133&134 (1985) 268.
- [16] H. Atsumi, S. Tokura, T. Yamauchi, S. Yamanaka and M. Miyake, *J. Nucl. Mater.* 141&143 (1986) 258.
- [17] W. Möller, B.M.U. Scherzer and J. Ehrenberg, *J. Nucl. Mater.* 111/112 (1982) 669.